

Quantum-limited amplification without instability

A. Metelmann,^{1,2,3,*} O. Lanes,⁴ T-Z. Chien,⁴ A. McDonald,^{5,6} M. Hatridge,⁴ and A. A. Clerk⁵

¹*Dahlem Center for Complex Quantum Systems and Fachbereich Physik,
Freie Universität Berlin, 14195 Berlin, Germany*

²*Institute for Theory of Condensed Matter, Karlsruhe Institute of Technology, 76131 Karlsruhe, Germany*

³*Institute for Quantum Materials and Technology,
Karlsruhe Institute of Technology, 76344 Eggenstein-Leopoldshafen, Germany*

⁴*Department of Physics and Astronomy, University of Pittsburgh, Pittsburgh, PA 15260, USA*

⁵*Pritzker School of Molecular Engineering, University of Chicago, 5640 S. Ellis Ave., Chicago, IL 60637, USA*

⁶*Department of Physics, University of Chicago, 5720 S. Ellis Ave., Chicago, IL 60637, USA*

(Dated: August 2, 2022)

Quantum parametric amplifiers typically generate by operating in proximity to a point of dynamical instability. We consider an alternate general strategy where quantum-limited, large-gain amplification is achieved without *any* proximity to a dynamical instability. Our basic mechanism (involving dynamics that conserves the number of squeezed photons) enables the design of a variety of one and two mode amplifiers that are not limited by any fundamental gain-bandwidth constraint. We focus on a particular realization that allows us to realize an ideal single-mode squeezing operation *in transmission*, and which has zero reflection. We present both a thorough theoretical analysis of this system (including pump-depletion effects), and also discuss results of an experimental superconducting quantum circuit implementation.

PACS numbers: 84.30.Le 03.65.Ta, 42.50.Pq 42.50.Lc

I. INTRODUCTION

Parametric amplifiers having quantum-limited noise properties play a crucial role in a variety of quantum information technologies. In optical-domain systems, they are a crucial resource for preparing both discrete-variable and continuous-variable entangled states [1]. For superconducting microwave circuits, quantum parametric amplifiers harnessing Josephson nonlinearities serve as a workhorse for fast, high-fidelity qubit measurements. Given the crucial role they play, there has been an enormous amount of activity (especially in the microwave-domain) looking at alternate amplifier designs that provide advantages in terms of bandwidth, noise and isolation (i.e. in-built non-reciprocity) (see e.g. Refs. [2–22]). Almost all these strategies ultimately use parametric processes that induce dynamical instability: in the absence of external dissipation or additional nonlinearities, the internal intra-cavity system dynamics would lead to unbounded exponential growth. This instability is cut-off by dissipation (i.e. the coupling to input and output transmission lines), and the underlying instability physics is used to generate the desired amplification. This basic paradigm is at the heart of standard degenerate and non-degenerate parametric amplifier designs (see [23, 24] for pedagogical reviews), as well as more complex amplifier designs.

While undeniably powerful, the strategy of harnessing an instability has some inherent drawbacks. As we discuss, it necessarily leads to a fundamental gain-

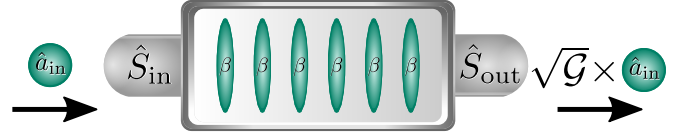


FIG. 1: Photons entering the Bogoliubov amplifier at the input port are converted into Bogoliubov quasiparticles via the squeezing transformation \hat{S}_{in} . When leaving the amplifier they are converted back to photons via the inverse squeezing transformation \hat{S}_{out} . Crucially, $\hat{S}_{\text{out}} \neq \hat{S}_{\text{in}}^{-1}$, results in the enhancement of the photon amplitude with factor $\sqrt{\mathcal{G}} > 1$.

bandwidth trade-off: amplification is achieved by tuning pump parameters closer and closer to instability, which correspondingly increases the system’s response time. This is analogous to the phenomenon of critical slowing down that occurs when one approaches a second-order phase transition. The net result is a system bandwidth that scales inversely with the square-root of the amplifier’s power gain [23, 24].

Here, we present an extremely general way to achieve ideal quantum limited amplification that does not involve proximity to a dynamical instability. The basic idea is to exploit what at first glance seems a very sub-optimal situation: use parametric processes that are effectively detuned from resonance. Such systems are described by mean-field Hamiltonians that are fully stable even without any external dissipation. They still however can generate remarkably ideal quantum-limited amplification: in particular, even though they use at most two photonic cavity modes, they are *fundamentally not subject to any gain-bandwidth constraints*. As we discuss, this is a direct consequence of the eigenstates of these systems being *squeezed photons*. Such squeezed photons are described

*Corresponding author: anja.metelmann@kit.edu

by so-called Bogoliubov modes, bosonic annihilation operators that are generated by squeezing transformations acting on standard photonic creation and destruction operators. The class of dynamically-stable amplifiers we introduce here all have the feature of having a set of Bogoliubov modes whose number operators are conserved.

The heuristic operation of our class of amplifiers is sketched in Fig. 1. Photons enter the input port, and are effectively converted to Bogoliubov quasiparticles; this involves a squeezing transformation \hat{S}_{in} . These quasiparticles then have simple, number conserving dynamics. To leave the amplifier, these Bogoliubov quasiparticles are converted back to photons via a second squeezing transformation \hat{S}_{out} . Amplification is achieved by the simple fact that $\hat{S}_{\text{out}} \neq \hat{S}_{\text{in}}^{-1}$: there is a net squeezing-amplification transformation implemented on photons scattered by the amplifier.

Our schemes have the further advantage that by a simple parameter tuning, they can directly implement the enhanced bandwidth strategy of Ref. [18], where the frequency dependent gain is extremely flat near resonance. While Ref. [18] achieved this via the introduction of a secondary, optimized external impedance, in our systems, this bandwidth enhancement is in-built. Yet another advantage of these designs is an intrinsic resilience against pump-depletion effects, something that is a direct consequence of not operating in proximity to an instability.

We show that our strategy is extremely general, and discuss a variety of implementations. The simplest corresponds to new way to operate a standard single-cavity DPA such that there is no gain-bandwidth product; this is analyzed in Sec.II B. We focus most of our attention however on an even more novel setup: a two-mode, two-port amplifier that achieved a perfect DPA squeezing operation *in transmission*. Despite the presence of an extra mode compared to a standard DPA, this system nonetheless has quantum-limited performance (i.e. one quadrature is amplified noiselessly). It also has no gain-bandwidth limitation, and overcomes a key limitation of standard DPA: they operate in reflection, meaning that there is no intrinsic separation of amplifier input and output. A detailed analysis of this setup is presented in Sec.III A. We also show that this setup is amenable with current superconducting circuit technology: Sec.III B describes rests of an experimental implementation of this novel two-mode amplifier showing a bandwidth which is enhanced by over a factor of 6 compared to the standard setups. Note that previous work has explored the use of detuned parametric driving to realize quantum non-demolition dynamics, which conserves one or more photonic quadratures [25–27]. Such QND interactions are distinct from the ideas we present here; in particular such QND systems are on the cusp of instability (i.e. they cannot be diagonalized), whereas our systems are fully stable (i.e. described by diagonalizable Hamiltonians).

II. THE BASICS: SINGLE MODE BOGOLIUBOV-MODE AMPLIFIER

A. Recap of a standard DPA

We first recall the basics of a degenerate parametric amplifier (DPA) in the stiff-pump limit. The amplifier consists of a principle cavity with a weak nonlinear coupling to an auxiliary pump mode. By driving this mode strongly with an external pump at an appropriate frequency, one realizes a mean-field Hamiltonian of the form:

$$\hat{\mathcal{H}} = \Delta \hat{a}^\dagger \hat{a} + \frac{\nu}{2} (\hat{a}^\dagger \hat{a}^\dagger + \hat{a} \hat{a}). \quad (1)$$

We are working in a rotating frame set by the pump frequency. \hat{a} is the photon lowering operator for the signal mode, and Δ is the detuning of the pump from the cavity resonance frequency. ν is the effective parametric drive amplitude (determined by both the nonlinearity and pump amplitude). We assume without loss of generality that both Δ and ν are real and positive. Note that for $\Delta < \nu$, the DPA Hamiltonian given in Eq. 1 is unstable: it cannot be diagonalized, and in the absence of the dissipation it generates unbounded exponential growth, corresponding to a dynamical instability.

Coupling the system to an input-output waveguide with coupling rate κ makes the system dynamically stable as long as $\kappa/2 \geq \nu$. Gain is generated by approaching the point of instability, i.e. by increasing ν so it approaches $\kappa/2$ from below. Signals incident on the waveguide will be reflected with gain.

The frequency dependent gain is obtained via input-output theory [28] and yields for zero detuning ($\Delta = 0$)

$$\mathcal{G}[\omega] = \frac{\left(\frac{2\omega}{D}\right)^2 + \mathcal{G}_0}{\left(\frac{2\omega}{D}\right)^2 + 1}, \quad \sqrt{\mathcal{G}_0} = \frac{\frac{\kappa}{2} + \nu}{\frac{\kappa}{2} - \nu} \quad (2)$$

where $D = 2\kappa/(\sqrt{\mathcal{G}_0} + 1)$ serves as the effective bandwidth of the amplifier, defined here as the full width at half of the maximum gain. Only signals contained within a frequency range of approximately D around resonance will be significantly amplified. In the relevant case where the zero frequency power gain is very large $\mathcal{G}_0 \gg 1$, we have

$$D \approx \frac{2\kappa}{\sqrt{\mathcal{G}_0}} \implies D\sqrt{\mathcal{G}_0} \approx 2\kappa. \quad (3)$$

This encapsulates the fundamental gain/bandwidth product that limits conventional parametric amplifiers. If one wants to increase the peak gain, it is necessarily accompanied by a reduction in the operating bandwidth of the amplifier. This is a generic feature of any amplifier that generates gain by operating closer to a point of dynamical instability.

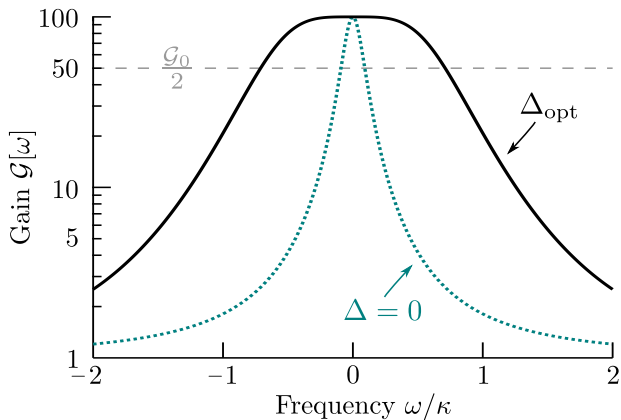


FIG. 2: Plot of the gain as a function of injected signal frequency for a zero frequency gain of 20dB. The optimally detuned Bogoliubov amplifier (ODBA) has a broad range of frequencies over which amplification occurs (solid black line). Conventional parametric amplifiers only amplify in a narrow range of frequencies (dotted teal line).

B. Optimally-detuned DPA: The ODBA

We now consider our DPA system in a case where the Hamiltonian is stable and diagonalizable. This requires $\Delta \geq \nu$. Here, the Hamiltonian can be diagonalized as

$$\hat{H} = \Lambda \hat{\beta}^\dagger \hat{\beta}, \quad \hat{\beta} = \cosh(r)\hat{a} + \sinh(r)\hat{a}^\dagger, \quad (4)$$

with $\Lambda = \sqrt{\Delta^2 - \nu^2}$ and where $\hat{\beta}$ is a canonical bosonic lowering operator in the Bogoliubov basis. The eigenstates of the Bogoliubov mode number operator $\hat{n}_r = \hat{\beta}^\dagger \hat{\beta}$ are squeezed Fock states $|n_r\rangle = \hat{S}(r)|n\rangle$ with $\hat{S}(r) = \exp[r/2(\hat{a}\hat{a} - \hat{a}^\dagger\hat{a}^\dagger)]$. The squeezing parameter r is given by $\tanh 2r = \nu/\Delta$. The dynamics of this Hamiltonian in the Bogoliubov basis are obviously stable and trivial. An input signal $\hat{\beta}_{\text{in}}$ injected into the waveguide would scatter as

$$\hat{\beta}_{\text{out}}[\omega] = e^{i\phi[\omega]}\hat{\beta}_{\text{in}}[\omega], \quad \phi[\omega] = 2\arg\left[i(\omega - \Lambda) + \frac{\kappa}{2}\right], \quad (5)$$

hence, the input in the Bogoliubov basis is just reflected with a phase $\phi[\omega]$. This phase is crucial to obtain any net amplification, which becomes obvious when considering the transformation back into the original frame

$$\begin{pmatrix} \hat{a}_{\text{out}}[\omega] \\ \hat{a}_{\text{out}}^\dagger[\omega] \end{pmatrix} = \mathcal{S}^{-1}(r) \begin{bmatrix} e^{+i\phi[\omega]} & 0 \\ 0 & e^{-i\phi[\omega]} \end{bmatrix} \mathcal{S}(r) \begin{pmatrix} \hat{a}_{\text{in}}[\omega] \\ \hat{a}_{\text{in}}^\dagger[\omega] \end{pmatrix}, \quad (6)$$

with the single mode squeezing transformation $\mathcal{S}(r)$

$$\begin{pmatrix} \hat{\beta} \\ \hat{\beta}^\dagger \end{pmatrix} = \mathcal{S}(r) \begin{pmatrix} \hat{a} \\ \hat{a}^\dagger \end{pmatrix}, \quad \mathcal{S}(r) = \begin{pmatrix} \cosh r & \sinh r \\ \sinh r & \cosh r \end{pmatrix}, \quad (7)$$

with $\mathcal{S}^{-1}(r)\mathcal{S}(r) = \mathbb{1}$. Crucially, the phase $\phi[\omega]$ ensures that the squeezing transformations do not cancel each

other out. This lack of cancellation results in net amplification of input signals.

To specify the parameters required for a single-mode Bogoliubov amplifier, we take the following operational approach. We imagine having a fixed decay rate κ , while being able to freely adjust the detuning Δ and drive ν . Changing both parameters is feasible in nearly all experimental platforms. We chose both such that the energy of the Bogoliubov mode matches the photonic loss rate

$$\sqrt{\Delta^2 - \nu^2} = \frac{\kappa}{2}. \quad (8)$$

The corresponding frequency dependent gain now reads

$$\mathcal{G}[\omega] = \frac{(\frac{2\omega}{D'})^4 + \mathcal{G}_0}{(\frac{2\omega}{D'})^4 + 1}, \quad (9)$$

where $D' = \sqrt{2}\kappa$ is the effective bandwidth of the optimally detuned Bogoliubov amplifier (ODBA). While superficially similar looking to the gain profile in Eq. (2) of a conventional DPA, the ODBA offers two distinct advantages. The first is that there is no gain-bandwidth limitation: the gain can be as large as desired without sacrificing bandwidth (see Fig. 2). The fact that the gain and bandwidth are independent is of enormous utility in experiments. The other distinct advantage of the ODBA is the relative flatness of the gain profile around zero frequency. In a standard DPA, the gain is only flat around an extremely narrow range of frequencies ω which satisfy $\omega \ll D$. In contrast, the gain of a ODBA is nearly constant around for frequencies ω near zero, with small leading order correction of the order $(\omega/D')^4$ (see Fig. 2)

The ODBA still maintains one of the main attractive features of a conventional DPA: it can be used as a quantum-limited amplifier without any added noise. Such amplifiers are required for several tasks related to quantum computation and communication. Our scheme is relevant in several experiment platforms, such as optical, microwave and mechanical setups. It is especially well suited for Josephson amplifiers used to readout superconducting quantum circuits. Finally, we stress that the ODBA is simple to implement experimentally. It does not require additional hardware, but relies instead on a carefully chosen choice of detuning and drive strength, both of which can be easily tuned in experiments.

III. AN IDEAL TWO-PORT SQUEEZER: THE TWO-MODE BOGOLIUBOV AMPLIFIER

The previous section showed how exploiting dynamics that conserved the number of squeezed photons (Bogoliubov excitations) in a simple parametrically driven cavity was enough to realize a quantum amplifier with exceptional properties. Here, we show how this basic idea becomes even more powerful in the setting of a two-cavity system.

A. The Optimally Imbalanced Parametric Amplifier: The OIBA

Parametric modulation of the coupling between two coupled cavity modes results in two basic interactions at the mean-field level: frequency conversion for modulating at the frequency difference of the mode pair, or parametric amplification if one drives at the sum of their frequencies. Our two-mode Bogoliubov amplifier utilizes resonant versions of these interactions simultaneously. We thus start with the mean-field Hamiltonian (rotating at the respective mode resonant frequencies)

$$\hat{\mathcal{H}} = G_1 \hat{d}_1^\dagger \hat{d}_2^\dagger + G_1^* \hat{d}_1 \hat{d}_2 + G_2 \hat{d}_1^\dagger \hat{d}_2 + G_2^* \hat{d}_1 \hat{d}_2^\dagger. \quad (10)$$

Here \hat{d}_n ($n \in 1, 2$) denotes the annihilation operator of mode n , and the coupling coefficients G_n contain the amplitude and the phase of two external modulation tones. With the latter we can control which quadratures of the modes are involved in the interaction.

Unlike the amplifier of Sec. II B, there is no explicit detuning term here. Nonetheless, our system can be made dynamically stable (even without any external dissipation) by constraining G_1 to be smaller than G_2 . In this regime, the intra-cavity dynamics of our system is yet again simply understood in terms of Bogoliubov modes whose total excitation number is conserved. Defining the squeezing parameter r via $\tanh 2r = G_1/G_2$, and introducing canonical Bogoliubov-mode lowering operators $\hat{\beta}_n = \hat{d}_n \cosh r + \hat{d}_n^\dagger \sinh r$, Eq. (10) takes the form

$$\hat{\mathcal{H}}_{\text{hop}} = \tilde{G} \hat{\beta}_1^\dagger \hat{\beta}_2 + h.c., \quad \tilde{G} = \sqrt{G_2^2 - G_1^2}. \quad (11)$$

Eq. (11) describes a simple hopping interaction that converts excitations between the local Bogoliubov modes at a frequency \tilde{G} . At first glance, this might seem to be of zero utility for amplification. This however misses the fact that when we now couple modes 1 and 2 to input-output transmission lines or waveguides, excitations enter and leave the system as photons, not as Bogoliubov excitations. This then provides a simple heuristic picture for our amplification mechanism as illustrated in Fig. 3: Input photons on mode 1 are converted to β_1 -mode excitations; this involves a single-mode squeezing transformation \hat{S}_{in} . The hopping interaction in Eq. (11) then converts the excitations to β_2 with a phase shift. The excitations in β_2 are then converted to photons in the transmission line coupled to mode 2; this involves a second single-mode squeezing transformation \hat{S}_{out} .

The above heuristic picture is borne out by an explicit calculation of the system's scattering matrix. Without loss of generality we take the coefficients G_1, G_2 to be real, and couple both cavity modes to external waveguides with symmetric coupling strengths $\kappa_n = \kappa$ (see Appendix C for the asymmetric case). From the Langevin equations of the system we find the eigenvalues of the dynamics

$$\epsilon_{1,2} = -\frac{\kappa}{2} \pm i\tilde{G}, \quad \tilde{G} \equiv \sqrt{G_2^2 - G_1^2}, \quad (12)$$

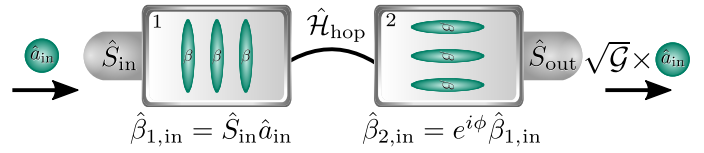


FIG. 3: Illustration of the operation mode of the OIBA. An input signal \hat{a}_{in} on mode 1 gets squeezed (\hat{S}_{in}), converted to a mode 2 Bogoliubov quasiparticle and undergoes a second squeezing transformation before leaving mode 2. Crucially, due to the conversion process between the modes the squeezing transformations do not cancel each other out and the output signal is amplified.

we see that if we choose $\tilde{G} = \kappa/2$, i.e., for optimally imbalanced interaction strengths $G_{1,2}$ in Eq. (10), we have a situation where the splitting of the system's normal modes is exactly equal to their width. As in Sec. II B, this matched-splitting operation leads to a number of exceptional properties, including an extremely flat gain versus frequency profile. We thus follow on this special tuning point in what follows.

The output for $\tilde{G} = \kappa/2$ yields in the Bogoliubov basis

$$\begin{bmatrix} \hat{\beta}_{1,\text{out}}[\omega] \\ \hat{\beta}_{2,\text{out}}[\omega] \end{bmatrix} = e^{i\phi[\omega]} \mathcal{P}^{-1} \begin{bmatrix} \cos \theta[\omega] & \sin \theta[\omega] \\ -\sin \theta[\omega] & \cos \theta[\omega] \end{bmatrix} \mathcal{P} \begin{bmatrix} \hat{\beta}_{1,\text{in}}[\omega] \\ \hat{\beta}_{2,\text{in}}[\omega] \end{bmatrix}. \quad (13)$$

The matrix operations here acting on the Bogoliubov input modes here have a simple interpretation. They correspond to the input excitation passing through a sequence of phase shifters. The corresponding frequency dependent beam-splitter angle, and phase shifter matrix are:

$$\theta[\omega] = \arcsin \left[\frac{4\omega^4}{\kappa^4} + 1 \right]^{-\frac{1}{2}}, \quad \mathcal{P} = \begin{pmatrix} -i & 0 \\ 0 & 1 \end{pmatrix}. \quad (14)$$

In addition we have an overall frequency-dependent phase shift

$$\phi[\omega] = \text{atan} \left[\frac{2\frac{\omega}{\kappa}}{1 - \frac{2\omega^2}{\kappa^2}} \right]. \quad (15)$$

The output of the mode $i = 1, 2$ contains now contributions from both modes, in contrast to the single-mode ODBA, where the input signal is simply reflected with a phase. This phase was the important ingredient to avoid the cancellation of the squeezing transformation, cf. Eq. 6. Here the situation is slightly different: to prevent the squeezing operations from canceling (hence generating amplification), the beam-splitter operation is now crucial. To see this we can consider the scattering behavior in the original mode-basis. and work in the basis of the orthogonal quadratures $\hat{X}_n = (\hat{d}_n + \hat{d}_n^\dagger)/\sqrt{2}$ and $\hat{P}_n = -i(\hat{d}_n - \hat{d}_n^\dagger)/\sqrt{2}$. The scattering matrix relating in-

put and output fields becomes ($\mathbf{X}_{\text{out}}[\omega] = \mathbf{s}[\omega]\mathbf{X}_{\text{in}}[\omega]$)

$$\begin{aligned} \mathbf{s}[\omega] &= e^{i\phi[\omega]} \mathcal{S}_Q^{-1}(r) \mathcal{B}(\theta[\omega]) \mathcal{S}_Q(r) \\ &= \frac{e^{i\phi[\omega]}}{\sqrt{\frac{4\omega^4}{\kappa^4} + 1}} \begin{pmatrix} \cot \theta[\omega] & 0 & 0 & -e^{-2r} \\ 0 & \cot \theta[\omega] & e^{2r} & 0 \\ 0 & -e^{-2r} & \cot \theta[\omega] & 0 \\ e^{2r} & 0 & 0 & \cot \theta[\omega] \end{pmatrix}, \end{aligned} \quad (16)$$

in the basis $\mathbf{X} = [\hat{X}_1, \hat{P}_1, \hat{X}_2, \hat{P}_2]^T$, and with the beam-splitter matrix

$$\mathcal{B}(\theta[\omega]) = \begin{bmatrix} \cos \theta[\omega] & 0 & \sin \theta[\omega] & 0 \\ 0 & \cos \theta[\omega] & 0 & \sin \theta[\omega] \\ -\sin \theta[\omega] & 0 & \cos \theta[\omega] & 0 \\ 0 & -\sin \theta[\omega] & 0 & \cos \theta[\omega] \end{bmatrix}, \quad (17)$$

and the squeezing transformation for the quadrature basis (absorbing the phase shift \mathcal{P})

$$\mathcal{S}_Q(r) = \frac{1}{\sqrt{2}} \begin{bmatrix} -ie^{+r} & e^{-r} & 0 & 0 \\ ie^{+r} & e^{-r} & 0 & 0 \\ 0 & 0 & e^{+r} & ie^{-r} \\ 0 & 0 & e^{+r} & -ie^{-r} \end{bmatrix}, \quad (18)$$

which describes local squeezing transformations. From the scattering matrix given in Eq.(16) it becomes clear that the beam-splitter prevents the cancellation of the squeezing transformations, with the net result being phase-sensitive amplification involving a frequency conversion process.

We already see the remarkable features of the amplifier: the reflections (diagonal elements) are zero on resonance ($\theta[0] = \pi/2$) and thus the system is perfectly impedance matched to its input ports. Moreover, the output of cavity 1 (2) contains the amplified P -quadrature and squeezed X -quadrature of cavity 2 (1), allowing for a separation of input and output ports for the signal. In contrast to single mode-squeezing, i.e., realized via the interaction $\mathcal{H}_s = \lambda \hat{d}^\dagger \hat{d}^\dagger + h.c.$, the squeezing/amplification here is also accompanied by a frequency conversion. Despite the fact that we use two degrees of freedom here (which might seem extraneous), we find that the amplification process is quantum-limited: it reaches the quantum-limit for phase-sensitive amplifiers of zero added noise [29].

Another crucial aspect of the optimally imbalanced Bogoliubov amplifier (OIBA) is the off-resonant gain behavior. Defining $\mathcal{G}_0 = e^{4r}$ as the zero-frequency power gain, we find for the gain as a function of frequency

$$\mathcal{G}[\omega] \equiv |s_{23}[\omega]|^2 = \frac{\mathcal{G}_0}{1 + \left[\frac{2\omega}{\mathcal{D}}\right]^4}, \quad \mathcal{D} = \sqrt{2}\kappa, \quad (19)$$

thus, the gain scales linearly with the (tunable) coupling strengths $G_{1,2}$, and the bandwidth over which amplification is possible is not affected by the amount of the gain, i.e., this amplifier is not limited by a fixed

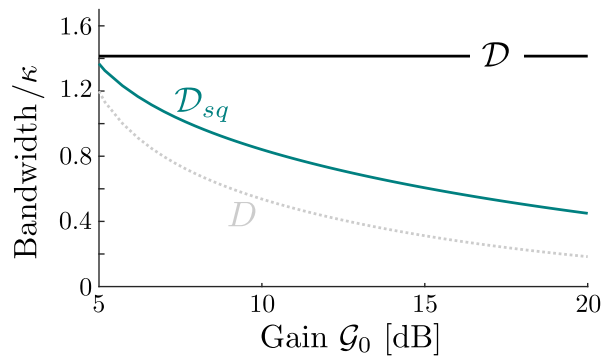


FIG. 4: Bandwidths for the OIBA as a function of the gain \mathcal{G}_0 . The black solid line depicts the amplification bandwidth $\mathcal{D} = \sqrt{2}\kappa$, which scales independently of the gain. This behavior does not translate to the squeezing bandwidth \mathcal{D}_{sq} (emerald solid line), which decreases for increasing gain. However, the \mathcal{D}_{sq} is enhanced compared to the squeezing bandwidth $D \simeq 2\kappa/\sqrt{\mathcal{G}_0}$ for the standard single mode setup (dotted grey line).

gain-bandwidth product. The resulting bandwidth is $\mathcal{D} = \sqrt{2}\kappa$, see Fig. 4.

An additional important question is whether this remarkable feature of a gain-independent bandwidth also manifests itself in the output squeezing. As discussed in Sec. II A, a conventional single-mode squeezer has an amplification bandwidth scaling with $D \simeq 2\kappa/\sqrt{\mathcal{G}_0}$, which coincides with the squeezing bandwidth. This squeezing bandwidth is defined as the frequency range over which the amount of squeezing is within 3 dB of the maximal on-resonance value. To determine the squeezing bandwidth for the Bogoliubov amplifier we consider the symmetrized output noise spectra of the X_1 -quadrature

$$\frac{\bar{S}_{X_1 X_1}[\omega]}{\bar{S}_{\text{SN}}} = \frac{1}{1 + \left[\frac{2\omega}{\mathcal{D}}\right]^4} \left(\left[\frac{2\omega}{\mathcal{D}}\right]^4 + \frac{1}{\mathcal{G}_0} \right). \quad (20)$$

with $\bar{S}_{\text{SN}} = 1/2$ as the shot-noise value. The first term describes vacuum fluctuation driving cavity 1, while the second term describes the squeezed cavity-2 noise. As discussed above, on resonance, i.e., $\omega = 0$, and $\bar{n}_2^T = 0$ the amount of squeezing scales inversely with the gain just as in a single-mode setup. However, the noise contribution from mode-1 becomes relevant for finite frequency; we find for the squeezing bandwidth $\mathcal{D}_{sq} \simeq \sqrt{2}\kappa(\mathcal{G}_0)^{-1/4}$. Hence the gain-independence of the amplification bandwidth does not translate to the squeezing bandwidth. However, it is notable that the squeezing bandwidth is enhanced compared to a single-mode setup, i.e., for the same gain value $\mathcal{G}_0 = \mathcal{G}_s \equiv \mathcal{G}$ we find $\mathcal{D}_{sq}/D \simeq \mathcal{G}^{1/4}/\sqrt{2}$. Note, without cavity-1 noise contribution in the spectrum $\bar{S}_{X_1 X_1}[\omega]$, the squeezing bandwidth would scale independently of the gain.

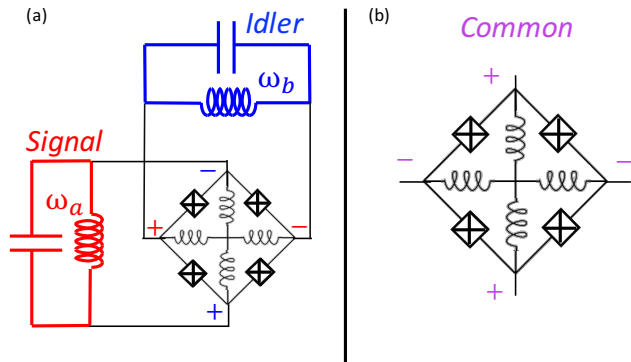


FIG. 5: (a) Signal (red) and Idler (blue) modes of a JPC connected to differential excitations of the central JRM. (b) The common mode of the JPC and JRM connects to both external modes and is typically used for pumping rather than signal input and output.

B. OIBA: Experimental Results

We demonstrate the power and functionality of these theoretical predictions using a shunted Josephson Parametric Converter (JPC) whose properties and fabrication are described in Ref. [8]. The core of this amplifier is a shunted Josephson Ring Modulator (JRM); a ring of four nominally identical Josephson junctions, shunted with linear inductors, as shown in Fig. 5. The ring is threaded with an external magnetic flux which creates three-wave mixing among the devices three modes.

The Hamiltonian of this device written in terms of the normal modes is

$$\begin{aligned}
 H_{JRM} = & -4E_J \left[\cos\left(\frac{\varphi_X}{2}\right) \cos\left(\frac{\varphi_Y}{2}\right) \cos(\varphi_Z) \cos\left(\frac{\varphi_{ext}}{4}\right) \right. \\
 & \left. + \sin\left(\frac{\varphi_X}{2}\right) \sin\left(\frac{\varphi_Y}{2}\right) \sin(\varphi_Z) \sin\left(\frac{\varphi_{ext}}{4}\right) \right] \\
 & + \frac{E_L}{4} (\varphi_X^2 + \varphi_Y^2 + 2\varphi_Z),
 \end{aligned} \tag{21}$$

where $E_L = \frac{\Phi_0^2}{L}$. We refer to these modes as the signal, idler, and common mode of the JRM. These mode excitations are again noted in Fig 5.

The four Josephson junctions on the outer arms of the JRM provide nonlinear couplings between the eigenmodes of the circuit [6]. Assuming that the ground state of the circuit is $\varphi_X = \varphi_Y = \varphi_Z = 0$ and it is stable as we tune the external magnetic flux bias, we can expand the nonlinear coupling terms around this ground state and make appropriate substitutions to rewrite the Hamiltonian in terms of the raising and lowering operators, up to 3rd order, as in [30, 31]

$$\hat{H}_{JPC} = \hat{H}_0 + g_3 (\hat{a} + \hat{a}^\dagger)(\hat{b} + \hat{b}^\dagger)(\hat{c} + \hat{c}^\dagger), \tag{22}$$

where \hat{H}_0 denotes the Hamiltonian of the three uncoupled modes and the g_3 term represents the strength of

the 3-wave mixing that gives rise to the gain and conversion processes in the JRM [12]. These 3-wave processes are then driven with a far off-resonance stiff tone to create effective two-body interactions. Note that the expansion of the cosine potentials also results in higher order terms that have been neglected, as they have significantly smaller magnitude. These terms will nonetheless hinder performance compared to the ideal 3-wave mixing Hamiltonian.

To achieve the Optimally Imbalanced Bogoliubov Amplifier (OIBA) experimentally, we start with two pump tones (one each at the sum and difference frequencies of the signal and idler modes) which drive the conversion and gain processes of the JPC with identical coupling rates. From here, the conversion tone amplitude is increased so that a large dip in signal reflection becomes visible. Then, we switch the read-out scheme to transmission, using a mixer to undo the amplifier's frequency conjugation so that we can compare same-frequency input and outputs in a Vector Network Analyzer.

To increase the gain, \mathcal{G} , both pumps are both now individually increased slowly at the same rate. As long as the dip in reflection is still present in reflection, the correct ratio of the pumps is approximately maintained.

If we compare the response of the OIBA to a more standard non-degenerate amplification process using a single pump tone, we can see that both scattering parameters of the OIBA are superior. The ≈ 10 dB dip in Fig. 6 b. means that the amplifier is still approximately matched in reflection. The OIBA is still bi-directional, meaning that one can amplify both from the signal to the idler mode, but also in reverse. A fully directional amplifier is still necessary to achieve ideal practical operation, because stray photons can still end up traveling backwards down the amplification chain to the qubit [13, 32]. Thus, in the OIBA measurements should still be performed with external isolators to protect the device being measured.

While the broad gain peak in transmission is not an ideal 20 dB, it has all the qualitative features predicted by theory, including the much larger bandwidth, flat peak, and phase-sensitive mode of amplification. At this bias point the single gain pump achieves only about 5 MHz bandwidth at this gain, which is typical for a standard Josephson Parametric Amplifier. The OIBA on the other hand, has a bandwidth of ≈ 33 MHz. Theory predicts an even broader bandwidth for the OIBA, but that rests upon having $\kappa_{sig} = \kappa_{idl}$, a condition that was slightly violated here ($\kappa_{sig} = 25$ MHz, $\kappa_{idl} = 20$ MHz). In addition, it was experimentally difficult to reach 20 dB gain in this mode of amplification on this amplifier due to unwanted higher order terms. In the future, this difficulty could be alleviated by using a more ideal mixing element, such as an array of SNAILs, with suppressed higher-order terms.

Despite these caveats, we stress that this experimental device still serves proving the validity of the basic concept. The crucial observation is the ratio of band-

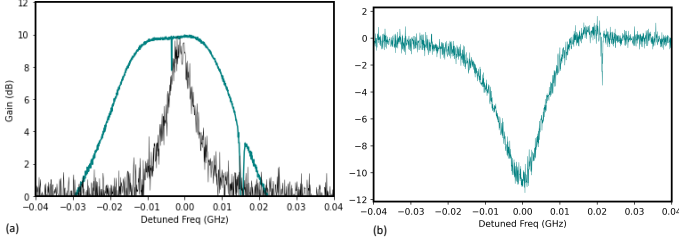


FIG. 6: (a) OIBA-pumped amplifier (teal) transmission gain versus frequency, compared to a more standard amplification setup using a single pump tone (black); in both cases we have 10 dB of gain in reflection. The OIBA scheme exhibits a dramatic improvement in bandwidth for the same amount of gain. (b) The reflection scattering parameter of the OIBA amplifier versus frequency, showing that there is almost perfect impedance matching on resonance (i.e. almost vanishing reflection).

widths between the two kinds of amplifier modes: the new OIBA scheme always yields a far larger bandwidth than the typical single-pump amplification setup (for the same external flux conditions). Further, the OIBA approach does not suffer from a gain-bandwidth product limit that constraints the standard single-pump approach to amplification.

C. OIBA: Pump-Depletion

We now show that the OIBA scheme has another strong advantage over more conventional approaches: it is more robust against pump depletion effects. In the former section we have seen that OIBA amplifier can be realized in a superconducting-circuit setup which uses a JPC as the mixing element, and which is driven via two external microwave tones. The relevant 3-wave mixing process is described via the Hamiltonian

$$\hat{\mathcal{H}}_{3W} = g_1 \hat{a}_1 \hat{d}_1^\dagger \hat{d}_2^\dagger + g_2 \hat{a}_2 \hat{d}_1^\dagger \hat{d}_2 + h.c.. \quad (23)$$

here \hat{a}_n denote the pump modes which are driven strongly at frequencies $\omega_{P,1} = \omega_1 + \omega_2$ and $\omega_{P,2} = \omega_1 - \omega_2$ (and detuned from their resonance). Performing a displacement transformation $\hat{a}_n \rightarrow a_n e^{-i\omega_{P,n}t - i\varphi_n} + \delta\hat{a}_n$, we can decompose the pump modes into their classical amplitudes a_n and corresponding fluctuations $\delta\hat{a}_n$. The pump phases φ_n will determine which quadrature-quadrature coupling we obtain. In general one assumes stiff pump modes, i.e., one sets $\hat{a}_n = \langle \hat{a}_n \rangle$ and neglects $\delta\hat{a}_n$, then the resonant interaction simplifies to Eq. (10) with $G_n = g_n \langle \hat{a}_n \rangle e^{-i\varphi_n}$.

The stiff pump approximation breaks down for larger input signal power. Here backaction effects on the pump become relevant and limit the dynamical range of the parametric amplifier. To go beyond the stiff pump approximation we derive the equations of motion for the

pump modes' expectation values

$$\begin{aligned} \frac{d}{dt} \langle \hat{a}_1 \rangle &= -\frac{\gamma_1}{2} \langle \hat{a}_1 \rangle - \sqrt{\gamma_1} a_{1,\text{in}} - ig_1 \langle \hat{d}_1 \hat{d}_2 \rangle, \\ \frac{d}{dt} \langle \hat{a}_2 \rangle &= -\frac{\gamma_2}{2} \langle \hat{a}_2 \rangle - \sqrt{\gamma_2} a_{2,\text{in}} - ig_2 \langle \hat{d}_1 \hat{d}_2^\dagger \rangle, \end{aligned} \quad (24)$$

where $\gamma_{1,2}$ denote the damping of the pump modes and $a_{1,2,\text{in}}$ correspond to the amplitude of the respective pump tone. The coupling to the correlators $\langle \hat{d}_1 \hat{d}_2^{(\dagger)} \rangle$ in the equations for the pump modes describe the backaction effects, the latter would be neglected under a stiff pump approximation. We evaluate the correlators on a mean-field level [7] and define

$$\begin{aligned} \Sigma_{1,\text{eff}} &\equiv i \frac{g_1}{\langle a_1 \rangle} \langle \hat{d}_1 \hat{d}_2 \rangle = \frac{\gamma_{1,\text{eff}}}{2} + i\Omega_{1,\text{eff}}, \\ \Sigma_{2,\text{eff}} &\equiv i \frac{g_2}{\langle a_2 \rangle} \langle \hat{d}_1 \hat{d}_2^\dagger \rangle = \frac{\gamma_{2,\text{eff}}}{2} + i\Omega_{2,\text{eff}}, \end{aligned} \quad (25)$$

with the effective damping rates

$$\begin{aligned} \gamma_{1,\text{eff}} &= + \frac{\gamma_1}{2} \frac{\sqrt{\mathcal{C}_1}}{[1 + \mathcal{C}_+ \mathcal{C}_-]^2} \left\{ \frac{X_{n,\text{in}}^2}{\bar{n}_{1,\text{in}}} \mathcal{C}_+ - \frac{P_{n,\text{in}}^2}{\bar{n}_{1,\text{in}}} \mathcal{C}_- \right\} + \gamma_{1,\text{eff}}^{\text{vac}}, \\ \gamma_{2,\text{eff}} &= \mp \frac{\gamma_2}{2} \frac{\sqrt{\mathcal{C}_2}}{[1 + \mathcal{C}_+ \mathcal{C}_-]^2} \left\{ \frac{X_{n,\text{in}}^2}{\bar{n}_{2,\text{in}}} \mathcal{C}_+ + \frac{P_{n,\text{in}}^2}{\bar{n}_{2,\text{in}}} \mathcal{C}_- \right\}, \end{aligned} \quad (26)$$

with $\mathcal{C}_\pm = \sqrt{\mathcal{C}_2} \pm \sqrt{\mathcal{C}_1}$, the cooperativities $\mathcal{C}_n = 4G_n^2/\kappa^2$, and where the minus sign in $\gamma_{2,\text{eff}}$ refers to an input in cavity 1. The damping rate associated with vacuum fluctuations driving mode-1 reads

$$\gamma_{1,\text{eff}}^{\text{vac}} = \frac{2g_1^2}{\kappa} \frac{1}{1 + \mathcal{C}_+ \mathcal{C}_-}, \quad (27)$$

which is negligible as it neither scales with the input signal nor the gain. In addition, the frequency shifts yield

$$\Omega_{n',\text{eff}} = (-1)^{n'+1} \frac{\gamma_{n'}}{2} \frac{\sqrt{\mathcal{C}_1 \mathcal{C}_2}}{[1 + \mathcal{C}_+ \mathcal{C}_-]^2} \frac{X_{n,\text{in}} P_{n,\text{in}}}{\bar{n}_{n',\text{in}}}, \quad (28)$$

which become only relevant if we have an input signal simultaneously in both quadratures, i.e., $X_{n,\text{in}}$ and $P_{n,\text{in}}$. Note, determining all backaction effects requires a self-consistent calculation, i.e., the cooperativities appearing in the expression for the effective decay rates $\gamma_{n,\text{eff}}$ and the frequency shifts $\Omega_{n,\text{eff}}$ depend on the pump amplitude and vice versa.

Including the backaction onto the pump modes we have now pump amplitudes which depend as well on the phase of the input signal, a situation which deviates from a standard single-tone (phase-insensitive) parametric amplifier. The latter case would be recovered by setting $\mathcal{C}_2 = 0$ in the upper expressions. Note that the OIBA requires a fine tuning of the pump amplitudes: for optimal performance the matching condition $\bar{G} = \kappa/2$ has to be achieved. Including pump depletion effects, one has a potential problem, as now, increases in the input

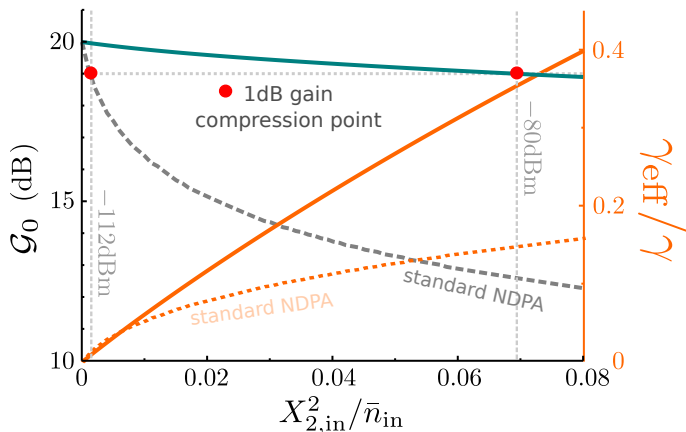


FIG. 7: Gain saturation pump-mode backaction effects in the OIBA amplifier, as a function of the input signal strength $X_{2,\text{in}}^2/\bar{n}_{\text{in}}$, where \bar{n}_{in} denotes the average number of pump photons required to obtain 20dB of gain. All numerical results were obtained self-consistently. For comparison the effective damping and the depleted gain for a standard parametric amplifier are plotted as well [grey dashed/orange dotted line]. Parameters are $\gamma_1/\kappa = \gamma_2/\kappa = 12$ and $g_1/\kappa = g_2/\kappa = 0.014$. Taking typical JPC-parameters from Ref. [7] the 1 dB compression point for the Bogoliubov amplifier is shifted by 32 dBm in comparison to the standard paramp [explicit values denoted in graph].

signal strength could cause one to violate the matching condition. To quantify this effect we define

$$\mathcal{C}_{1,2}(\gamma_{1,\text{eff}}, \gamma_{2,\text{eff}}) \equiv \mathcal{C}_{n,\text{eff}} = \frac{\mathcal{C}_n}{(1 + \bar{\gamma}_{n,\text{eff}})^2} \equiv \mathcal{C}_n \chi_n \quad (29)$$

as the effective cooperativities with $\bar{\gamma}_{n,\text{eff}} = \gamma_{n,\text{eff}}/\gamma_n$ and \mathcal{C}_n denoting the undisturbed cooperativities, i.e., $\mathcal{C}_n = \mathcal{C}_{n,\text{eff}}$ for $\chi_n = 1$. The alteration of the cooperativities affects the matching condition for the OIBA amplifier, and we define the deviation from the optimal matching as $\delta\mathcal{C} = \mathcal{C}_{2,\text{eff}} - \mathcal{C}_{1,\text{eff}} - 1$. Assuming $\chi_n \approx \chi$ the deviation can be approximated as $\delta\mathcal{C} \approx \chi - 1$ and thus can be assumed to be small. The effect of this mismatch is a minor back-reflection of the input signal, e.g. for the example in Fig. 7 around 0.04% of the signal are reflected at the 1dB compression point of the amplifier.

To analyze the back-action effects further we consider the situation where an input is injected in the X-quadrature of the second cavity. The effective decay rates in Eq. 26 can be approximated as

$$\gamma_{n,\text{eff}} \approx \frac{\gamma_n}{16} \mathcal{G}_{\text{eff}} \frac{X_{2,\text{in}}^2}{\bar{n}_{n,\text{in}}}, \quad (30)$$

thus, the effective decay rates scale linearly with the effective power gain \mathcal{G}_{eff} and the input signal. This coincides with the scaling for the standard parametric amplifier (for $\mathcal{C}_2 = 0$) [7], leading to gain saturation if the input signal strength is increased for constant gain. In a standard parametric amplifier the effective gain saturation

scales as

$$\sqrt{\frac{\mathcal{G}_{PA,\text{eff}}}{\mathcal{G}_{PA}}} = \frac{1}{\sqrt{\mathcal{G}_{PA}}} \frac{\chi^{-1} + \mathcal{C}}{\chi^{-1} - \mathcal{C}} \approx 1 - \sqrt{\mathcal{G}_{PA}} \bar{\gamma}_{\text{eff}} \quad (31)$$

with $\mathcal{G}_{PA} = (1 + \mathcal{C})^2/(1 - \mathcal{C})^2$ and the approximation in the second step holds for small effective decay rates. Crucially, the reduction of the gain is enhanced by the amplitude gain in this standard parametric amplifier.

Taking that the OIBA effective decay rates in Eq.(30) scale linearly with the effective gain, we should at first side expect similar saturation effects in the OIBA. The effective decay rates are even enhanced compared to the standard case, see Fig. 7. Importantly, the enhanced decay rates do not mean that the gain saturates earlier. In contrast, the effective decay rates are enhanced because the effective gain is larger, see Fig. 7. This originates in the modified scaling of the gain with the pump amplitude. The OIBAs effective gain saturation scales as

$$\sqrt{\frac{\mathcal{G}_{0,\text{eff}}}{\mathcal{G}_0}} = \frac{2\sqrt{\chi}}{\chi + 1} \approx 1 - \frac{\bar{\gamma}_{n,\text{eff}}^2}{2} \quad (32)$$

where we approximated $\chi_n \approx \chi$ and expanded the resulting expression for small effective decay rates. Clearly, this is a much favorable scaling, as the reduction of the gain is not enhanced by a gain-factor. This explains why the saturation of the OIPA sets in for much higher input signal strength, cf. Fig. 7. This robustness should hold true for similar amplifiers without a gain-bandwidth product, where the gain scales directly with the pump amplitude.

IV. THE CLASS OF BOGOLIUBOV AMPLIFIERS

The previous sections have established a general principle for realizing amplification without instability, by using table Hamiltonians in the Bogoliubov basis. We now show that these ideas can be further generalized to a wide class of multi-mode systems. We consider N Bogoliubov modes which obey the stable dynamics

$$\hat{\mathcal{H}} = \sum_{i,j=1}^N \lambda_{i,j} \hat{\beta}_i^\dagger \hat{\beta}_j, \quad (33)$$

with coupling strength $\lambda_{i,j}$. The Bogoliubov modes $\hat{\beta}_n$ are obtained via the general squeezing transformation

$$\hat{S}_n = e^{R_{n,m}(\hat{a}_n \hat{a}_m - \hat{a}_n^\dagger \hat{a}_m^\dagger)}, \quad R_{n,m} = \frac{r_n}{1 + \delta_{n,m}}, \quad (34)$$

acting on the cavity mode operators $\hat{a}_{n,m}$ in the unsqueezed basis, i.e., $\hat{\beta}_n = \hat{S}_n^\dagger \hat{a}_n \hat{S}_n$. Here $\delta_{n,m}$ denotes the Kronecker delta. The squeezing transformation corresponds to either single-mode squeezing ($n = m$) or two-mode squeezing ($n \neq m$). The squeezing parameter r_n

depends on parameters in the respective unsqueezed cavity basis and are specified case by case. We can consider now two different classes containing a phase-sensitive and a phase-insensitive version each: namely the class of detuned Bogoliubov amplifiers and the class of imbalanced Bogoliubov amplifiers.

1. Detuned Bogoliubov amplifiers

We start with the detuned Bogoliubov amplifiers, they are obtained by setting $\lambda_{ij} = \delta_{ij}\lambda$ in Eq. (33), so that the Hamiltonian in the Bogoliubov basis reduces to

$$\hat{\mathcal{H}} = \lambda \sum_{i=1}^N \hat{\beta}_i^\dagger \hat{\beta}_i. \quad (35)$$

For $n = m$, i.e., single-mode squeezing, and $N = 1$ we have only a single Bogoliubov mode and recover the ODBA discussed in Sec II B. This means that by setting $\lambda = \sqrt{\Delta^2 - \nu^2}$ we obtain the phase-sensitive amplifier described by the Hamiltonian in Eq. (1) in the unsqueezed cavity basis. However, it is also possible to design a phase-insensitive version via a two-mode squeezing transformation, i.e., for $n \neq m$ and the two Bogoliubov modes $\hat{\beta}_n = \cosh r \hat{a}_n + \sinh r \hat{a}_m^\dagger$ with $n, m = 1, 2$. The squeezing parameter yields then $\tanh 2r = G/\Delta$, while the Bogoliubov mode energy becomes $\lambda = \sqrt{\Delta^2 - G^2}$. Here the detuning Δ and the two-mode squeezing strength G are defined in the original basis as

$$\hat{\mathcal{H}} = \Delta \left(\hat{a}_1^\dagger \hat{a}_1 + \hat{a}_2^\dagger \hat{a}_2 \right) + G \left[\hat{a}_1^\dagger \hat{a}_2^\dagger + \hat{a}_1 \hat{a}_2 \right]. \quad (36)$$

Thus we simply have a detuned two-mode squeezing interaction among two cavity modes, in analogy to the ODBA, which involves a detuned single-mode squeezing interaction. Note that both kinds of detuned Bogoliubov amplifiers realize amplification without instability when the energy of the Bogoliubov mode matches the photonic loss rate, i.e., $\lambda = \kappa/2$ as done in Eq. (8). Thus, by simply detuning the standard single or two-mode squeezing interactions the amplification process is stabilized and the resulting bandwidth is independent of the gain.

2. Imbalanced Bogoliubov amplifiers

A second approach to achieving amplification using stable dynamics is to have a Hamiltonian that describes hopping interactions between localized Bogoliubov modes. Considering the simplest case of two modes and $i \neq j$ in Eq. (33) the Hamiltonian in the Bogoliubov base becomes

$$\hat{\mathcal{H}} = \lambda \left(\hat{\beta}_1^\dagger \hat{\beta}_2 + \hat{\beta}_1 \hat{\beta}_2^\dagger \right), \quad (37)$$

which corresponds to a swapping of excitation between the modes, i.e., the number of Bogoliubov quasiparticles is conserved and they coherently oscillate back and

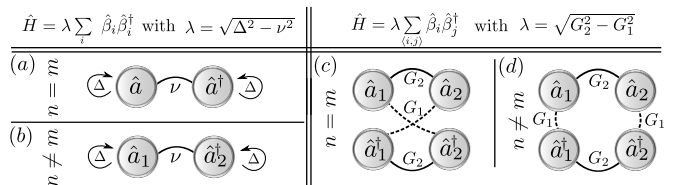


FIG. 8: The class of one and two-mode Bogoliubov amplifiers in the unsqueezed cavity basis. Configurations (a,c) realize phase-sensitive amplification without an instability, while the configurations (b,d) correspond to the phase-insensitive counterpart. In sketch (c,d) G_1 denotes single- or two-mode squeezing in (d) and (c) respectively, while G_2 corresponds to a hopping interaction.

forth between the modes β_1 and β_2 . Based on this stable dynamics in the Bogoliubov basis we can repeat our protocol to obtain phase-sensitive ($n = m$) and phase-insensitive amplification ($n \neq m$) without instability.

Figure 8(c,d) depict sketches of the required configurations of the imbalanced Bogoliubov amplifiers in the unsqueezed basis. We find that in addition to single- or two-mode squeezing interactions with strength G_1 , we require a hopping interaction between the cavity modes 1 and 2 associated with strength G_2 in this original basis. The sweet spot of operating without an instability is obtained for $\lambda = \sqrt{G_2^2 - G_1^2} = \kappa/2$. Hence we refer to this class as the imbalanced Bogoliubov amplifiers, as the interaction strengths of the involved processes have to be imbalanced to match this condition. Note that the bosonic Kitaev chain amplifier introduced in [33] can be viewed as a multi-mode realization of this kind of amplifier.

V. CONCLUSION

We have presented a novel class of quantum-limited amplifiers which operate effectively detuned from any instability. This mode of operation brings in the remarkable features of no gain-bandwidth limitation and a very flat frequency-gain profile. We showed that the removal of the instability is best understood in the basis of Bogoliubov modes undergoing stable dynamics. Crucially, the transformations of an input signal into and out of the Bogoliubov basis are distinct and do not cancel each other out, leading to net amplification of the input signal. A theoretical analysis on the level of a mean-field ansatz shows that such Bogoliubov amplifiers are potentially more robust to detrimental backaction effects induced by large input signals. We introduced in detail the optimally imbalanced Bogoliubov amplifier (OIBA), which is based on a imbalanced frequency conversion and parametric amplification process. The OIBA, for which we presented proof-of-principle experimental results, is an amplifier operating in transmission and is perfectly impedance-matched to its input ports. These features make it an interesting candidate for a cascaded amplifier

architecture, and for further applications to quantum signal processing.

VI. ACKNOWLEDGEMENTS

AM acknowledges funding by the Deutsche Forschungsgemeinschaft through the Emmy Noether program (Grant No. ME 4863/1-1) and the project CRC 910. AAC and AM acknowledge support from the Air Force Office of Scientific Research under Award No. FA9550-19-1-0362, and the Army Research Office under Grant No. W911NF-19-1-0328. OL, TZC, and MJH acknowledge support from the Army Research Office under Grant No. W911NF-18-1-0144 and the National Science Foundation under Grant No. PIRE-1743717.

Appendix A: Squeezing properties

We can parametrize the squeezing obtained in the Bogoliubov amplifier via the squeezing parameter r , defined via the ratio $e^{-2r} = \bar{S}_{X_n X_n}[0]/\bar{S}_{\text{SN}}$ with $\bar{S}_{\text{SN}} = 1/2$ as the shot-noise value and $\bar{S}_{X_n X_n}[0]$ denotes the symmetrized output noise of the X_n -quadratures. Here both quadratures, X_1 and X_2 , are squeezed symmetrically hence we use only one squeezing parameter r , with $e^{-2r} = 1/\mathcal{G}_0$ for a pure vacuum input. For the latter case the squeezed output light is pure. This changes once an input in mode- n is accompanied by thermal fluctuations originating from a bath with average occupation \bar{n}_n^T . For example, considering an input on cavity-2, the impurity of the output light of cavity-1 can be quantified by an effective thermal occupancy

$$\bar{n}_{\text{eff}} = \sqrt{\bar{S}_{X_1 X_1}[0]\bar{S}_{P_1 P_1}[0]} - \frac{1}{2} = \bar{n}_2^T, \quad (\text{A1})$$

i.e., the output light is just as impure as the input light, which coincides with the situation for a single-mode squeezing setup.

Appendix B: QND amplifier

For a balanced choice of coupling parameters in the Hamiltonian given in Eq. (10), i.e., $G_1 = G_2 = G \in \mathbb{R}$, we obtain a quantum nondemolition (QND) interaction [34], i.e., both X-quadratures commute with the resulting Hamiltonian:

$$\hat{\mathcal{H}}_{\text{QND}} = 2G\hat{X}_1\hat{X}_2. \quad (\text{B1})$$

Such a process corresponds to a non-disturbing measurement of the X-quadratures of each mode, where the P-quadratures obtain the information of the X-quadratures, which themselves are not affected by the measurement. The combined balanced gain and conversion process realize a phase-sensitive amplifier, whose nonreciprocal version was briefly introduced in our former work [19]. Crucially, as the X-quadratures are not affected by the QND-interaction no squeezing of an input signal is possible and the amplifier cannot be impedance matched on its input port.

The scattering matrix in the quadrature basis $\mathbf{X} = [\hat{X}_1, \hat{P}_1, \hat{X}_2, \hat{P}_2]^T$ becomes

$$\mathbf{s}[\omega] = e^{i\phi} \begin{pmatrix} -1 & 0 & 0 & 0 \\ 0 & -1 & \sqrt{\mathcal{G}[\omega]} & 0 \\ 0 & 0 & -1 & 0 \\ \sqrt{\mathcal{G}[\omega]} & 0 & 0 & -1 \end{pmatrix}, \quad \mathcal{G}[\omega] = \frac{\mathcal{G}_Q}{\left[1 + \frac{4\omega^2}{\kappa^2}\right]^2} \quad (\text{B2})$$

with $\mathbf{X}_{\text{out}}[\omega] = \mathbf{s}[\omega]\mathbf{X}_{\text{in}}[\omega]$ and the phase $\phi = 2 \arg[\kappa + 2i\omega]$. The frequency dependent gain $\mathcal{G}[\omega]$ contains the zero-frequency amplitude gain $\sqrt{\mathcal{G}_Q} = 8G/\kappa$. Here the P-quadratures contain the amplified X-quadratures

of the respective other mode, where for gain we require $G > \kappa/8$. Note, although the scattering matrix in this basis seems somewhat asymmetric, we still have a reciprocal amplifier. Transforming back to the non-hermitian basis of d_n operators we obtain a completely symmetric scattering matrix. The QND amplifier has as well no gain-bandwidth limit, but the bandwidth of $D_{QND} = \sqrt{\sqrt{2} - 1}\kappa$ is half as large as for the OIBA.

To determine the added noise for the QND-amplifier we calculate the symmetrized noise spectral density and obtain for the added noise (referred back to the input)

$$\bar{n}_{\text{add}} = \frac{1}{\bar{G}_Q} \left(\frac{1}{2} + \bar{n}^T \right), \quad (\text{B3})$$

here \bar{n}^T denotes the thermal bath which the cavity receiving the input signal is coupled to. Clearly we can reach the quantum limit for large gain, even at finite temperature.

Appendix C: Influence of asymmetries

In this section we briefly discuss the influence of asymmetries in the decay rates of the two cavity modes ($\kappa_1 \neq \kappa_2$), as well as deviations from the optimal matching condition. Starting with the eigenvalues of the system

$$\epsilon_{1,2} = -\frac{\kappa_{\pm}}{2} \pm i\sqrt{\tilde{G}^2 - \frac{\kappa_{\pm}^2}{4}}, \quad \kappa_{\pm} = \frac{\kappa_1 \pm \kappa_2}{2}, \quad (\text{C1})$$

with $\tilde{G} = \sqrt{G_2^2 - G_1^2}$ as used in the main text. Thus, although we have asymmetric decay, we can still extract the point of optimally imbalanced parametric processes, which is obtained for the condition

$$\tilde{G} = \frac{\sqrt{\kappa_+^2 + \kappa_-^2}}{2}, \quad \epsilon_{1,2} = \frac{\kappa_{\pm}}{\sqrt{2}} e^{\pm i\frac{\pi}{4}}. \quad (\text{C2})$$

The scattering matrix in the quadrature basis becomes

$$\mathbf{s}[\omega] = \begin{pmatrix} \mathcal{R}_-[\omega] & 0 & 0 & \mathcal{T}_-[\omega] \\ 0 & \mathcal{R}_-[\omega] & \mathcal{T}_+[\omega] & 0 \\ 0 & \mathcal{T}_-[\omega] & \mathcal{R}_+[\omega] & 0 \\ \mathcal{T}_+[\omega] & 0 & 0 & \mathcal{R}_+[\omega] \end{pmatrix}, \quad (\text{C3})$$

with the reflections and transmissions

$$\begin{aligned} \mathcal{R}_{\pm}[\omega] &= -\frac{\mathcal{C}_1 - \mathcal{C}_2 + \left[1 \mp i\frac{2\omega}{\kappa_1}\right] \left[1 \pm i\frac{2\omega}{\kappa_2}\right]}{\mathcal{C}_2 - \mathcal{C}_1 + \left[1 - i\frac{2\omega}{\kappa_1}\right] \left[1 - i\frac{2\omega}{\kappa_2}\right]}, \\ \mathcal{T}_{\pm}[\omega] &= +\frac{2\left[\sqrt{\mathcal{C}_1} \pm \sqrt{\mathcal{C}_2}\right]}{\mathcal{C}_2 - \mathcal{C}_1 + \left[1 - i\frac{2\omega}{\kappa_1}\right] \left[1 - i\frac{2\omega}{\kappa_2}\right]}, \end{aligned} \quad (\text{C4})$$

with the cooperativities $\mathcal{C}_n = 4G_n^2/(\kappa_1\kappa_2)$. On resonance the transmission and reflection coefficients become

$$\mathcal{R}_{\pm}[0] = \frac{\Delta_{\mathcal{C}}}{\Delta_{\mathcal{C}} + 2}, \quad \mathcal{T}_{\pm}[0] = +\frac{2\left[\sqrt{\mathcal{C}_1} \pm \sqrt{\mathcal{C}_2}\right]}{\Delta_{\mathcal{C}} + 2}, \quad (\text{C5})$$

with the definition $\Delta_{\mathcal{C}} = [\mathcal{C}_2 - \mathcal{C}_1 - 1]$, so we can characterize the deviations from the matching condition for the Bogoliubov amplifier as $\Delta_{\mathcal{C}} \neq 0$. The reflection always vanishes for $\Delta_{\mathcal{C}} = 0$, corresponding to the impedance matching condition $\tilde{G} = \sqrt{\kappa_1\kappa_2}/2$. Note, the point of optimal imbalance, corresponding to $\Delta_{\mathcal{C}} = 2\kappa_-^2/(\kappa_1\kappa_2)$, and the impedance matching condition only coincide for symmetric decay rates. The gain $|\mathcal{T}_+[0]|^2$ increases with the cooperativities as long as $\Delta_{\mathcal{C}} \geq -1$. For $-2 < \Delta_{\mathcal{C}} < -1$ the denominator is smaller than one and thus the resulting gain is enhanced and the reflected signal starts to get become amplified as well.

-
- [1] C. Weedbrook, S. Pirandola, R. García-Patrón, N. J. Cerf, T. C. Ralph, J. H. Shapiro, and S. Lloyd, *Rev. Mod. Phys.* **84**, 621 (2012), URL <https://link.aps.org/doi/10.1103/RevModPhys.84.621>.
- [2] M. A. Castellanos-Beltran, K. D. Irwin, G. C. Hilton, L. R. Vale, and K. W. Lehnert, *Nat Phys* **4**, 929 (2008).
- [3] M. Malnou, D. A. Palken, L. R. Vale, G. C. Hilton, and K. W. Lehnert, *Phys. Rev. Applied* **9**, 044023 (2018).
- [4] N. Bergeal, F. Schackert, M. Metcalfe, R. Vijay, V. E. Manucharyan, L. Frunzio, D. E. Prober, R. J. Schoelkopf, S. M. Girvin, and M. H. Devoret, *Nature* **465**, 64 (2010).
- [5] N. Bergeal, R. Vijay, V. E. Manucharyan, I. Siddiqi, R. J. Schoelkopf, S. M. Girvin, and M. H. Devoret, *Nat Phys* **6**, 296 (2010).
- [6] B. Abdo, F. Schackert, M. Hatridge, C. Rigetti, and M. Devoret, *App. Phys. Lett.* **99**, 162506 (2011).
- [7] B. Abdo, A. Kamal, and M. Devoret, *Phys. Rev. B* **87**, 014508 (2013).
- [8] T.-C. Chien, O. Lanes, C. Liu, X. Cao, P. L. and S. Motz, G. Liu, D. Pekker, and M. Hatridge, arXiv:1903.02102 (2019).
- [9] C. Macklin, K. O'Brien, D. Hover, M. E. Schwartz, V. Bolkhovskiy, X. Zhang, W. D. Oliver, and I. Siddiqi, *Science* **350**, 307 (2015).
- [10] V. V. Sivak, S. Shankar, G. Liu, J. Aumentado, and M. H. Devoret, arXiv:1909.08005 (2019).
- [11] B. Abdo, K. Sliwa, L. Frunzio, and M. Devoret, *Phys. Rev. X* **3**, 031001 (2013).
- [12] K. M. Sliwa, M. Hatridge, A. Narla, S. Shankar, L. Frunzio, R. J. Schoelkopf, and M. H. Devoret, *Phys. Rev. X* **5**, 041020 (2015).
- [13] F. Lecocq, L. Ranzani, G. A. Peterson, K. Cicak, R. W. Simmonds, J. D. Teufel, and J. Aumentado, *Phys. Rev. Appl.* **7**, 024028 (2017).

- [14] A. Kamal and A. Metelmann, *Phys. Rev. Applied* **7**, 034031 (2017).
- [15] L. Mercier de Lépinay, E. Damskäg, C. F. Ockeloen-Korppi, and M. A. Sillanpää, *Phys. Rev. Applied* **11**, 034027 (2019).
- [16] F. Lecocq, L. Ranzani, G. A. Peterson, K. Cicak, A. Metelmann, S. Kotler, R. W. Simmonds, J. D. Teufel, and J. Aumentado, arXiv:1909.12964 (2019).
- [17] A. Metelmann and A. A. Clerk, *Phys. Rev. Lett.* **112**, 133904 (2014).
- [18] T. Roy, S. Kundu, M. Chand, A. M. Vadiraj, A. Ranadive, N. Nehra, M. P. Patankar, J. Aumentado, A. A. Clerk, and R. Vijay, *Appl. Phys. Lett.* **107**, 262601 (2015).
- [19] A. Metelmann and A. A. Clerk, *Phys. Rev. X* **5**, 021025 (2015).
- [20] C. F. Ockeloen-Korppi, E. Damskäg, J.-M. Pirkkalainen, T. T. Heikkilä, F. Massel, and M. A. Sillanpää, *Phys. Rev. X* **6**, 041024 (2016).
- [21] A. Metelmann and A. A. Clerk, *Phys. Rev. A* **95**, 013837 (2017).
- [22] Q. Zhong, S. Ozdemir, A. Eisfeld, and A. M. and R. El-Ganainy, arXiv:1904.13005 (2019).
- [23] A. A. Clerk, M. H. Devoret, S. M. Girvin, F. Marquardt, and R. J. Schoelkopf, *Rev. Mod. Phys.* **82**, 1155 (2010).
- [24] A. Roy and M. Devoret, *Comptes Rendus Physique* **17**, 740 (2016), ISSN 1631-0705, quantum microwaves / Micro-ondes quantiques, URL <https://www.sciencedirect.com/science/article/pii/S1631070516300640>.
- [25] A. Szorkovszky, G. A. Brawley, A. C. Doherty, and W. P. Bowen, *Phys. Rev. Lett.* **110**, 184301 (2013).
- [26] A. Szorkovszky, A. Clerk, A. Doherty, and W. Bowen, *New Journal of Physics* **16**, 063043 (2014).
- [27] A. Szorkovszky, A. Clerk, A. Doherty, and W. Bowen, *New Journal of Physics* **16**, 043023 (2014).
- [28] C. W. Gardiner and M. J. Collett, *Phys. Rev. A* **31**, 3761 (1985).
- [29] C. M. Caves, *Phys. Rev. D* **26**, 1817 (1982).
- [30] F. D. O. Schackert, Ph.D. thesis, Yale University (2013).
- [31] C. Liu, T.-C. Chien, M. Hatridge, and D. Pekker, *Phys. Rev. A* **101** (2020).
- [32] W.-A. Li, G.-Y. Huang, and Y. Chen, *J. Opt. Soc. Am. B* **36**, 306 (2019), URL <http://josab.osa.org/abstract.cfm?URI=josab-36-2-306>.
- [33] A. McDonald, T. Pereg-Barnea, and A. A. Clerk, *Phys. Rev. X* **8**, 041031 (2018), URL <https://link.aps.org/doi/10.1103/PhysRevX.8.041031>.
- [34] V. B. Braginsky, Y. I. Vorontsov, and K. S. Thorne, *Science* **209**, 547 (1980), <http://www.sciencemag.org/content/209/4456/547.full.pdf>.